HHS Public Access

Author manuscript

J Neuromuscul Dis. Author manuscript; available in PMC 2019 September 09.

Published in final edited form as:

J Neuromuscul Dis. 2018 ; 5(3): 295–306. doi:10.3233/JND-180323.

Mineralocorticoid Receptor Antagonists in Muscular Dystrophy Mice During Aging and Exercise

Jeovanna Lowe[a], **Feni K. Kadakia**[a], **Jonathan G. Zins**[a], **Michael Haupt**[a], **Kyra K. Peczkowski**[a], **Neha Rastogi**[a], **Kyle T. Floyd**[a], **Elise P. Gomez-Sanchez**[b], **Celso E. Gomez-Sanchez**[c], **Mohammad T. Elnakish**[a,d], **Jill A. Rafael-Fortney**[a,1,*], **Paul M.L. Janssen**[a,1]

[a]Department of Physiology & Cell Biology, College of Medicine, The Ohio State University, Columbus, OH, USA

[b]Department of Pharmacology & Toxicology, University of Mississippi Medical Center, Jackson, MS, USA

[c]Department of Internal Medicine, University of Mississippi Medical Center, Jackson, MS, USA

[d]Department of Pharmacology & Toxicology, Faculty of Pharmacy, Helwan University, Cairo, Egypt

Abstract

Background: Mineralocorticoid receptor antagonists added to angiotensin converting enzyme inhibitors have shown pre-clinical efficacy for both skeletal and cardiac muscle outcomes in young sedentary dystrophin-deficient *mdx* mice also haploinsufficient for utrophin, a Duchenne muscular dystrophy (DMD) model. The *mdx* genotypic DMD model has mild pathology, making non-curative therapeutic effects difficult to distinguish at baseline. Since the cardiac benefit of mineralocorticoid receptor antagonists has been translated to DMD patients, it is important to optimize potential advantages for skeletal muscle by further defining efficacy parameters.

Objective: We aimed to test whether therapeutic effects of mineralocorticoid receptor antagonists added to angiotensin converting enzyme inhibitors are detectable using three different reported methods of exacerbating the *mdx* phenotype.

Methods: We tested treatment with lisinopril and the mineralocorticoid receptor antagonist spironolactone in: 10 week-old exercised, 1 year-old sedentary, and 5 month-old isoproterenol treated *mdx* mice and performed comprehensive functional and histological measurements.

Results: None of the protocols to exacerbate *mdx* phenotypes resulted in dramatically enhanced pathology and no significant benefit was observed with treatment.

Conclusions: Since endogenous mineralocorticoid aldosterone production from immune cells in dystrophic muscle may explain antagonist efficacy, it is likely that these drugs work optimally during the narrow window of peak inflammation in *mdx* mice. Exercised and aged *mdx* mice do not display prolific damage and inflammation, likely explaining the absence of continued efficacy

*Correspondence to: Jill A. Rafael-Fortney, Department of Physiology & Cell Biology, College of Medicine, The Ohio State University, 410 Hamilton Hall, 1645 Neil Avenue. Columbus, OH 43210, USA. Tel.: +1 614 292 7043; rafaelfortney.1@osu.edu.
[1]These authors contributed equally

CONFLICT OF INTEREST

The authors declare no conflict of interest relevant to this study.

of these drugs. Since inflammation is more prevalent in DMD patients, the therapeutic window for mineralocorticoid receptor antagonists in patients may be longer.

Keywords

Mineralocorticoid receptors; Duchenne muscular dystrophy; spironolactone; lisinopril; mdx mice

INTRODUCTION

Over the past three decades the average lifes-pan of patients with Duchenne muscular dystrophy (DMD) has increased due to increased use of ventilatory support and prophylactic antibiotics, which help prevent fatal respiratory infections due to weakened respiratory muscles [1-4]. Since DMD affects all striated muscles, this lengthened lifespan has resulted in the unmasking of cardiomyopathy in a majority of patients and an increase in fatalities resulting from heart failure [5, 6]. Glucocorticoids are currently used as a standard-of-care for DMD to improve ambulation, but have many serious side-effects including potential adverse effects on the heart [2, 7-11]. Most recently, genetic therapies using an exon-skipping approach to target the gene encoding dystrophin, which is mutated in DMD, are starting to become available. However, these therapies restore only a truncated version of dystrophin, are applicable for only a subset of mutations, and do not currently show promise to target the heart. Therefore, therapies that have the potential to target pathogenic events common to dystrophic skeletal muscles and the heart, may further improve lifespan and quality of life for DMD patients.

A few years ago, we tested whether prophylactic use of mineralocorticoid receptor (MR) antagonists, used commonly in late stage heart failure, when added to standard-of-care angiotensin converting enzyme inhibitors (ACEi) for early cardiomyopathy, were able to alleviate the early signs of cardiomyopathy in a DMD mouse model. We showed that this drug combination was able to improve functional and histological features of both the heart and skeletal muscles [12]. The cardiac efficacy of MR antagonists added to standard-of-care was then demonstrated in DMD patients [13, 14].

Since MR had not previously been reported to be present in skeletal muscles, the preclinical efficacy of MR antagonists demonstrated for dystrophic skeletal muscles was unexpected. Therefore, we have conducted further preclinical studies to optimize the potential use of MR antagonists for skeletal muscle pathology in addition to beginning to define the molecular mechanisms of their action. We have now demonstrated that specific and non-specific MR antagonists work with equivalent efficacy for dystrophic skeletal muscles and heart, but that ACEi alone does not improve functional parameters [15, 16]. We have also shown that MR are present in skeletal muscles, that dystrophic skeletal muscles contain high levels of 11β-hydroxysteroid dehydrogenase 2 that provides pre-receptor specificity for aldosterone to the MR and that MR functions as a steroid hormone receptor in human myotubes and in mouse muscles leading to transcriptional changes in up to 200 genes [17-19]. Surprisingly, myeloid cells present in regions of muscle damage in dystrophic mouse models contain high levels of aldosterone synthase, the rate limiting final enzyme required for aldosterone production [20]. This local production of aldosterone during muscle damage would explain the

effectiveness of MR antagonists for dystrophic skeletal muscles, since neither DMD patients nor mice have increased levels of circulating aldosterone secreted by the adrenal glands [20].

The original and several follow-up efficacious preclinical studies were conducted in 20 week-old sedentary dystrophin-deficient *mdx* mice also haploinsufficient for utrophin, which develop quantitatively more skeletal and cardiac muscle fibrosis than *mdx* mice. One preclinical study in 20 week-old sedentary *mdx* mice did not show sufficient deficits in many *mdx* parameters to measure therapeutic improvements. In this study, we aimed to test whether therapeutic effects of MR antagonists added to ACEi were able to be detected using 3 different previously reported methods of exacerbating the mild *mdx* phenotype [21-29]. We therefore tested treatment with the ACEi lisinopril and the MR antagonist spironolactone in 10 week-old exercised *mdx* mice, 1 year-old sedentary *mdx* mice and 5 month-old isoproterenol treated *mdx* mice.

MATERIALS AND METHODS

Mice, treatment, and study design

All mouse studies were conducted under a protocol approved by the institutional laboratory animal care and use committee. The Exercised *mdx* study contained 24 C57BL/10 *mdx* male mice with 12 untreated and 12 treated from 4–10 weeks-of-age with water bottles containing both lisinopril (132 mg/l) and spironolactone (250 mg/l) (LS) replaced 3 times per week to provide approximate dosages of 20 and 37.5 mg/kg × day, respectively. All mice were then run on a treadmill twice per week from 6–10 weeks using the TREAT-NMD protocol DMD_M.2.1.001 (as detailed below). At 10 weeks-of-age, outcome measures included forelimb grip strength, *in vitro* force measurements of *extensor digitorum longus* (EDL) and diaphragm, in addition to immunoglobulin G (IgG) staining of heart, quadriceps, *tibiallis anterior* (TA), soleus and fibronectin staining of diaphragm as previously described [15]. IgG staining of TA muscles also included samples from an additional 12 untreated sedentary 10 week-old *mdx* males and 5 untreated sedentary 10 week-old C57BL/10 males.

The Aged *mdx* study consisted of 36 *mdx* males with 18 untreated and 18 treated from 4 to 52 weeks-of-age with LS delivery and dosages as described above, and 18 untreated C57BL/10 male mice bred in house with breeders originally purchased from Harlan. At 1 year-of-age, outcomes included grip strength, echocardiography, an exhaustion treadmill running test, *in vitro* force measurements of EDL and diaphragm, IgG staining of heart, quadriceps, diaphragm, and abdominal muscles.

The Isoproterenol *mdx* study contained 20 *mdx* males with 10 untreated and 10 treated from 4 weeks to 5 months-of-age with LS delivery and dosages as described above, and 10 untreated C57BL/10 male mice. At 5 months-of-age, all mice were injected intraperitoneally with 200 μg/g Evan's Blue Dye and then 24 hours later with 500 μg/g isoproterenol ((–)-Isoproterenol hydrochloride, Sigma #I650) [30] every 2 hours for a total of 3 dosages as in Standard Operating Procedure for "Mouse heart Evan's blue dye uptake assay" (www.parentprojectmd.org/research/for-researchers-industry/resources/standard-operating-procedures-for-duchenne-animal-models/). A second group of *mdx* males were either treated with the beta-blocker metoprolol ($n = 11$) at a dosage of 2.5 mg/kg × day (17 mg/l) using

water bottle delivery as described above for LS or left untreated ($n = 5$), and then both treated with Evan's Blue Dye and isoproterenol as above. Mice were sacrificed 2 hours after the final isoproterenol administration, hearts were excised and frozen in optimal cutting temperature (OCT) in liquid-nitrogen cooled isopentane, cryosectioned, and stained for IgG. Both IgG and Evan's Blue Dye staining as a percentage of the entire transverse ventricular section were quantified.

Treadmill running

For the Exercised *mdx* study, mice began exercise treatment on a six lane Exer 6M treadmill (Columbus Instruments) at 6 weeks of age and continued until sacrifice at 10 weeks of age. A Plexiglas plate prevented mice from touching the electric shock grid during all running bouts. If a mouse stopped running and hit the Plexiglas plate, the touch was usually enough of a stimulus for the mouse to begin running again. If a mouse continually hit the plate, the experimenter gently touched the mouse with a paintbrush to prompt running. Mice were run horizontally (i.e. 0 degree angle) for 30 minutes twice a week at 12 m/min, with either 2 or 3 days rest in between bouts. Each exercise period began with an additional 3-minute session at 8 m/min to acclimatize the mice. Up to three mice were put in a single lane for exercise, with care taken to ensure all mice were continually running. If a mouse needed excessive prodding to run, the treadmill was stopped and the mice were given a short break of a few seconds. Once the break was complete, the treadmill was started again to complete a total, but sometimes interrupted, 30 minutes of exercise. Mouse 6398 showed fatigue during 4 running bouts; mouse 6380 showed fatigue during 2 running bouts; mouse 6397, 6431, and 6429 each showed fatigue during 1 running bout; mouse 6411 showed fatigue during the last running bout only. Running was performed by an individual blinded to treatment.

For the Aged *mdx* study, a subset of the one-year-old mice (6 LS treated *mdx*; 6 untreated *mdx*; and 6 C57BL/10) underwent an exhaustion treadmill running test performed by an individual blinded to genotype and treatment. A total of 6 mice were placed on the treadmill, one per lane, and were run in horizontal orientation. The electric shock grid at the back of the treadmill remained off as described above. Each day, running was performed at the same time of day, with housing conditions and feeding state remaining constant to limit variability. Groups of 6 mice were removed from their living units by a different individual than the one performing the treadmill test, randomized and coded. On the first day of training, all mice ($n = 18$) were run for 10 minutes at 9 m/min. On the second day of training, all mice were run for 6 minutes at 9 m/min, and then the speed was increased by 1 m/min each minute until a total of 10 minutes was reached. On the third day of training, the mice were run for 6 minutes at 9 m/min, and then the speed was increased by 1 m/min each minute until 12 total minutes had elapsed. On testing day, the treadmill was started at 9 m/min for 5 minutes, after which the speed was increased by 1 m/min each minute until exhaustion. Once the speed reached 35 m/min, it was capped to avoid measuring maximal running speed instead of exhaustion. When a mouse became exhausted, the treadmill and stopwatch were stopped for a few seconds, the mouse was removed and placed back in its cage, and the treadmill and stopwatch were then reengaged. This process was continued until all 6 mice in the cohort became exhausted and were removed. A mouse was considered exhausted when it refused to run for 10 consecutive seconds after repeated gentle nudges.

Grip strength measurements

For the Exercised *mdx* study, forelimb grip strength was measured before the first exercise treatment and ~48 hours after the last exercise treatment. The first investigator separated mice into unmarked cages, randomly selected a mouse to be given to the second investigator, who remained blinded to the treatment groups and performed the grip strength procedure. The mice were held by their tails so that their front paws were able to grip a wire attached to a force transducer, then swiftly and uniformly pulled backwards until the clasp was broken. This procedure was repeated three times with one minute rests between measurements. The highest value of the three was reported as maximal grip strength. The weight of each mouse was recorded at both time points. All measurements were performed by the same individual to limit experimental variability.

For the Aged *mdx* study, grip strength tests were designed to measure maximal grip strength and also determine whether untreated or treated mice show muscle fatigue using a similar technique as described above, but with additional repeated trials. Mice were trained for two sessions mimicking the conditions on the third session where measurements were recorded. Five series of five pulls each with a pause of 1 minute in between the series were performed. The highest value in the first trial was taken as the peak force produced from rested mice and the highest value in the fifth trial was taken as the peak force produced in fatigued mice. As described above, all measurements were performed blinded by the same individual.

In vivo cardiac measurements

On the day of sacrifice, the body weight of each mouse was recorded and resting, non-anesthetized, non-invasive electrocardiographic recordings were taken using the ECGenie system (Mouse Specifics Inc.) as previously reported [15]. Analysis of QT-interval, heart rate (HR), as well as QT adjusted for HR variability (QTc) was done using time intervals when paws were in contact with the electrodes and HR remained consistent.

In vivo left ventricular contractile function was evaluated using a high-frequency ultrasound imaging system (VEVO 2100,VisualSonics,Toronto,ON,Canada) as previously described [31]. Mice were anesthetized with isoflurane at a concentration of 2% and then maintained at 1.0%. The measurements were taken from the parasternal short-axis view in M-mode. Analysis was performed using VisualSonics Cardiac Measurements Package by an investigator blinded to treatment.

Ex vivo EDL and diaphragm contraction force measurements

All data was collected and analyzed by individuals blinded to genotype and treatment. For the Aged *mdx* study, the EDL muscle from each leg was carefully exposed under a dissection microscope. Two pieces of suture were used to tie a knot on each tendon. The muscles were secured by tying 5–8 additional knots and then the EDL was removed from the leg. For the Exercised *mdx* study (for all groups in that study) the EDL muscle was dissected and removed from the leg first, and then sutures were placed. A modified Krebs-Henseleit solution (with BDM, and 0.25 mM $CaCL_2$) was applied to the muscle throughout the dissection process. The sutures were tied around the tendons on each end of the muscle so that knots could be placed over two hooks (one attached to a force transducer, the other a

linear micromanipulator) in a muscle bath through which oxygenated Krebs-Henseleit (without BDM and 2.0 mM $CaCl_2$ added) at 30°C was continuously cycled. This multi-knot attachment method removes any attachment compliance and ensures that all length changes are directly reflecting changes in the muscle length. Muscles were stretched to optimal length using twitch contractions (evoked by a single 4 ms pulse) as previously described [15]. After 10 minutes, a tetanus contraction was performed (150 Hz for 250 ms). For the Aged *mdx* study, after another 5 min rest period, 6 eccentric (ECC) contractions (150 Hz for 450 ms, subjected to a 3% stretch for the final 200 ms of contraction) were done with five minutes of rest between the first 5 stimulations and 15 minutes of rest between the fifth and sixth stimulation as described [15]. Following force measurements, the sutures were removed and muscles weighed. Forces are expressed per unit of cross-sectional area (CSA). Force recordings and analyses were both done using custom-made LabView (National Instruments) programs. Diaphragm strips were carefully dissected and tetanic contractions as well as a fatigue protocol were performed as previously described [15].

Histopathology and quantification

For histological analyses muscles, as specified in the study designs above, were embedded in OCT medium and frozen on liquid-nitrogen cooled isopentane. Eight μm cryosections were stained with Hematoxylin and Eosin (H&E) to verify section quality or with an antibody against mouse IgG (Alexa 488 goat anti-mouse IgG, 1:200; Life Technologies) to quantify ongoing muscle damage as previously described [16]. TAs were also stained with rat anti-CD11b (1:50, BD Pharmingen; # 550282) to quantify the percentage of CSA with immune cell infiltration. Diaphragms were stained with rabbit anti mouse fibronectin (1:40, Abcam, ref# ab23750) or collagen I (1:200, Abcam, ref# ab34710) and detected with Alexa 555 goat anti rabbit IgG secondary antibody (1:200, Life Technologies, ref# A21429). Quantification of damage was performed using Adobe Photoshop and is reported as a percentage of CSA. Fibronectin quantification on diaphragm sections was performed using a tolerance of 30. Longitudinal quadriceps and diaphragm sections were excluded from analysis. IgG staining of soleus and heart from the Exercised *mdx* study were performed, but not quantified due to the absence of a quantifiable amount of damage. All histological quantification was conducted by an individual blinded to treatment and genotype. Quadriceps muscles from untreated year-old *mdx* mice from the Aged *mdx* study ($n = 3$) and 20 week-old untreated *utrn*$^{+/-}$;*mdx* from a previously published study [15] were stained with a rabbit polyclonal antibody against CYP11B2 after fixation with ice-cold acetone for 5 minutes and permeabilization with 0.75% saponin for 5 minutes [20], and then detected with Alexa 555 goat anti rabbit IgG secondary antibody (1:200, Life Technologies, ref# A21429) and counterstained with DAPI.

Data and statistical analysis

All data was included for statistical calculations after applying pre-determined exclusion criteria, which included forces below 30 mN/mm^2 for diaphragm tetanus and forces below 60 mN/mm^2 for EDL tetanus, or longitudinal samples for histological measurements. *n* for each parameter are shown in Tables 1 and 2. For the Aged *mdx* study, data was analyzed using one-way ANOVA. If the overall ANOVA indicated statistical significance, Dunnett's *post-hoc* test was used to test for significant differences between each group compared with

the untreated *mdx* group. For the Exercised *mdx* study, a Student's *t*-test was performed to test for differences between untreated and LS treated mice. For the Isoproterenol *mdx* study, data was analyzed using one-way ANOVA followed by Dunnett's *post-hoc* test to compare LS mice with untreated controls and wild-type mice studied in parallel. Metroprolol treated mice were compared using a Student's *t*-test with the separate cohort of untreated *mdx* controls treated in parallel with that group. Summary values for all data are presented as mean ± SE. *P* values ≤0.05 were accepted as significant.

RESULTS

In the Exercised *mdx* study, male *mdx* mice were treated with LS from 4 to 10 weeks-of-age or left untreated and then run on a treadmill for 30 minutes twice a week at 12 m/min according to the TREAD-NMD Standard-Operating-Procedure put in place to "Accelerate preclinical phase of new therapeutic treatment development" DMD_M.2.1.001: "Use of treadmill and wheel exercise for impact on *mdx* mice phenotype." Surprisingly, in our study, the exercise regime did not greatly exacerbate muscle damage or function compared to our previous baseline studies in sedentary *mdx* mice [9] (Table 1). The only parameter that appeared exacerbated was that of ongoing damage to TA muscle as measured by intracellular IgG accumulation with 10 ± 4% cross-sectional area in exercised *mdx* (Table 1) versus 5 ± 1% in a separate cohort of sedentary *mdx* males (Fig. 1). Treatment showed a non-significant positive trend towards improvement in this one parameter (4 ± 1% in LS treated exercised *mdx*) ($p = 0.1201$) (Table 1). There were no differences between untreated and LS treated exercised mice in the other parameters including forelimb grip strength, diaphragm specific force, EDL specific force, inflammation in the TA muscles, quadriceps damage, and diaphragm fibrosis content, which did not appear substantially different from our previous data on 10 week-old wild-type mice [16] (Table 1 and Fig. 1). Interestingly, out of the groups of 12 untreated and 12 LS treated mice, 5 untreated mice, but only 1 treated mouse, showed fatigue during at least 1 treadmill bout and required prodding with a paintbrush to encourage running.

In the Aged *mdx* study, we observed that exhaustion running was an excellent differentiator between 1 year-old C57 (870 ± 189.1 meters) and *mdx* (270 ± 25.1 meters) mice, but that this parameter was not improved by LS treatment (262 ± 46.9 meters) (Table 2). Forelimb grip strength of 1 year *mdx* mice is lower than that in younger dystrophic mice [15], but is not changed by treatment. There is however a non-statistically significant trend towards improvement in grip strength force per body weight in LS treated (30.1 ± 1.1 mN/g) compared to untreated (28.7 ± 1.2 mN/g) 1 year-old *mdx* mice (Table 2). A trend towards improvement from LS treatment was also observed on EDL force drop after the 5th eccentric contraction (ECC) with 73 ± 3% for LS versus 62 ± 6% for untreated and 79 ± 5% for C57 ($p = 0.0942$ by *t*-test comparing LS and untreated) and in diaphragm collagen content (55 ± 3% for LS versus 59 ± 2% for untreated (Table 2 and Fig. 2). LS treatment did not affect diaphragm specific force, diaphragm fatigue, EDL specific force, or quadriceps ongoing damage as measured by intracellular IgG in 1 year-old *mdx* mice (Table 2 and Fig. 2). No ongoing damage or quantitative cumulative damage was observed in *mdx* hearts even at this age. One year-old *mdx* mice still maintained normal heart function with an ejection fraction of 59.8 ± 2.5%, which was not affected by LS treatment (57.8 ± 2.7%).

For the isoproterenol *mdx* study we observed a wide variability of cardiac damage resulting from this beta-adrenergic stress in dystrophic mice and that IgG staining was easier to detect than Evan's blue dye (not shown). After isoproterenol stress, LS treated *mdx* males showed 16.9 ± 3.9% IgG positive ventricular cross-sectional area, compared to 14.9 ± 2.5% in untreated *mdx* males and 3.2 ± 1.3% in wild-type controls (Figs. 3A and 4A). ANOVA showed that isoproterenol stress increased damage in *mdx* mice ($p = 0.0034$), but Dunnett's *post-hoc* test showed no differences between untreated and LS treated *mdx* mice ($p = 0.8245$). We then tested whether a selective beta-1-blocker is sufficient to prevent the damage incurred from this isoproterenol induced beta-adrenergic stress. A second group of untreated *mdx* males treated with isoproternol in parallel with the metoprolol group exhibited an even lower amount of cardiac damage in response to beta-adrenergic stress (2.5 ± 1.2%). The metoprolol treated *mdx* group had an average of 7 ± 2.0% damage, which was not significantly different from the untreated group ($p = 0.3280$) (Figs. 3B and 4B).

To begin to understand why LS treatment in aged *mdx* mice did not show similar efficacy as previously observed repeatedly in 20 week-old sedentary dystrophin-deficient *mdx* mice also haploinsufficient for utrophin ("het mice"), we immunostained quadriceps sections from untreated *mdx* mice from the Aged *mdx* study with previously published [15] untreated het mice for the aldosterone synthase enzyme, CYP11B2. Based on qualitative scoring of quadriceps transverse sections, there appeared to be less ongoing inflammation with CYP11B2 positive myeloid cells in aged *mdx* muscles than 20 week-old het muscles (Fig. 5).

DISCUSSION

Overall, the effects of long-term LS treatment assessed at one year-of-age were minimal. However, this result is not completely surprising based on our recent mechanistic data. These data include that LS has a beneficial effect on stabilizing membrane integrity during ongoing damage early in the course of the disease [17], and myeloid inflammatory cells locally produce aldosterone in dystrophic muscles [20]. Aldosterone levels are increased within muscles during ongoing damage when large numbers of inflammatory cells are present and 11β-hydroxysteroid dehydrogenase 2 expression in dystrophic muscles results in MR selectivity for aldosterone [20]. Therefore, it is likely that spironolactone works by preventing this ongoing MR signaling from inflammatory cells. This hypothesis is consistent with the absence of high levels of circulating aldosterone in dystrophic mice or patients. Ongoing damage and high levels of inflammation are prevalent early in the disease pathogenesis in *mdx* mice, but become less prevalent as the mouse ages. Indeed, our data support that 20 week-old het muscles show more regions with aldosterone synthase positive myeloid cells than 1 year-old *mdx* muscles in this study, although future studies involving isolation and quantification of muscle immune cells from dystrophic models at different ages will be needed to confirm this hypothesis. Transient inflammation may explain the short-term improvements resulting from MR antagonism in dystrophic mice. In contrast, persistent inflammation is longer lasting in patients with Duchenne muscular dystrophy (DMD), where muscle damage is ongoing. Therefore, MR antagonists may show greater long-term efficacy in DMD patients than in mice. There is also the possibility that metabolism of lisinopril or spironolactone differs during aging and that resulting differences in exposure could alter the

effect of the drug's serum levels in 20 week-old and 1 year-old mice. This alternative explanation will be explored in the future in additional cohorts of mice.

The published standard-operating procedure on the "Use of treadmill and wheel exercise for impact on *mdx* mice phenotype" did not exacerbate the phenotype of young *mdx* mice in our studies compared to our previous studies of sedentary *mdx* mice and most phenotypes measured were very close to wild-type. Therefore, the statistical sensitivity for detecting improvements in young *mdx* due to treatment was low. Recent reports suggest that running protocols over a longer time-period further increase deficits in *mdx* mice [32]. However, the fatigue observed in more of the untreated *mdx* mice suggest the possibility of an effect of LS on muscle fatigue. In the future, a similar study, possibly carried out in the more severe "het" *utrn*$^{+/-}$; *mdx* model with additional incorporation of the running to exhaustion test, may provide more informative differential results between LS treated and untreated exercised mice.

Similarly, although published studies show more uniform increases in cardiac damage with the beta-adrenergic agonists dobutamine or isoproterenol in *mdx* mice [27, 33], cardiac damage in several *mdx* mice in our study did not appear to be greatly exacerbated compared to our previously published data for 5 month-old sedentary *mdx* mice [9] or wild-type C57 controls. Pre-mature collection of the tissues during peak injury hours may have impacted the degree of cardiac damage following isoproterenol injury and it is possible that longer time-points would improve differentiation between the groups. The presence of high levels of damage in a subset of untreated and treated *mdx* mice also suggests that LS treatment may not be sufficient to protect dystrophic hearts during times of stress and treatment with an additional beta-blocker should also be considered clinically. However, the follow-up test with a beta-blocker showed lower levels of ongoing damage in the untreated group of male isoproterenol *mdx* mice, suggesting that highly variable amounts of ongoing damage are present between *mdx* males and that isoproterenol stress from this protocol may only mildly contribute to the ongoing damage. This result would have positive connotations for patients, who may not show increased cardiac damage due to beta-adrenergic stress.

ACKNOWLEDGMENTS

This study was funded by DOD MD120063 and in part by NIH R01 NS082868 (to JRF). Echocardiography was performed using equipment in the OSU Small Animal Imaging Core.

REFERENCES

[1]. Birnkrant DJ, Bushby K, Bann CM, Alman BA, Apkon SD, Blackwell A, Case LE, Cripe L, Hadjiyannakis S, Olson AK, Sheehan DW, Bolen J, Weber DR, Ward LM. Diagnosis and management of Duchenne muscular dystrophy, part 2: Respiratory, cardiac, bone health, and orthopaedic management. Lancet Neurol. 2018;17:347–61. [PubMed: 29395990]

[2]. Birnkrant DJ, Bushby K, Bann CM, Apkon SD, Blackwell A, Brumbaugh D, Case LE, Clemens PR, Hadjiyannakis S, Pandya S, Street N, Tomezsko J, Wagner KR, Ward LM, Weber DR. Diagnosis and management of Duchenne muscular dystrophy, part 1: Diagnosis, and neuromuscular, rehabilitation, endocrine, and gastrointestinal and nutritional management. Lancet Neurol. 2018;17:251–67. [PubMed: 29395989]

[3]. Kieny P, Chollet S, Delalande P, Le Fort M, Magot A, Pereon Y, Perrouin Verbe B. Evolution of life expectancy of patients with Duchenne muscular dystrophy at AFM Yolaine de Kepper centre

between 1981 and 2011. Annals of Physical and Rehabilitation Medicine. 2013;56:443–54. [PubMed: 23876223]

[4]. Passamano L, Taglia A, Palladino A, Viggiano E, D'Ambrosio P, Scutifero M, Rosaria Cecio M, Torre V, F DEL, Picillo E, Paciello O, Piluso G, Nigro G, Politano L. Improvement of survival in Duchenne Muscular Dystrophy: Retrospective analysis of 835 patients. Acta Myol. 2012;31:121–5. [PubMed: 23097603]

[5]. McNally EM, Kaltman JR, Benson DW, Canter CE, Cripe LH, Duan D, Finder JD, Groh WJ, Hoffman EP, Judge DP, Kertesz N, Kinnett K, Kirsch R, Metzger JM, Pearson GD, Rafael-Fortney JA, Raman SV, Spurney CF, Targum SL, Wagner KR, Markham LW. Contemporary cardiac issues in Duchenne muscular dystrophy. Working Group of the National Heart, Lung, and Blood Institute in collaboration with Parent Project Muscular Dystrophy. Circulation. 2015;131:1590–8. [PubMed: 25940966]

[6]. Spurney CF. Cardiomyopathy of Duchenne muscular dystrophy: Current understanding and future directions. Muscle Nerve. 2011;44:8–19. [PubMed: 21674516]

[7]. Wei L, MacDonald TM, Walker BR. Taking glucocorticoids by prescription is associated with subsequent cardiovascular disease. Annals of Internal Medicine. 2004;141:764–70. [PubMed: 15545676]

[8]. Wong BL, Rybalsky I, Shellenbarger KC, Tian C, McMahon MA, Rutter MM, Sawnani H, Jefferies JL. Long-term outcome of interdisciplinary management of patients with duchenne muscular dystrophy receiving daily glucocorticoid treatment. The Journal of Pediatrics. 2017;182:296–303.e1. [PubMed: 28043681]

[9]. Janssen PM, Murray JD, Schill KE, Rastogi N, Schultz EJ, Tran T, Raman SV, Rafael-Fortney JA. Prednisolone attenuates improvement of cardiac and skeletal contractile function and histopathology by lisinopril and spironolactone in the mdx mouse model of Duchenne muscular dystrophy. PLoS One. 2014;9:e88360. [PubMed: 24551095]

[10]. Kim S, Zhu Y, Romitti PA, Fox DJ, Sheehan DW, Valdez R, Matthews D, Barber BJ. Associations between timing of corticosteroid treatment initiation and clinical outcomes in Duchenne muscular dystrophy. Neuromuscul Disord. 2017;27:730–7. [PubMed: 28645460]

[11]. Sali A, Guerron AD, Gordish-Dressman H, Spurney CF, Iantorno M, Hoffman EP, Nagaraju K. Glucocorticoid-treated mice are an inappropriate positive control for long-term preclinical studies in the mdx mouse. PLoS One. 2012;7:e34204. [PubMed: 22509280]

[12]. Rafael-Fortney JA, Chimanji NS, Schill KE, Martin CD, Murray JD, Ganguly R, Stangland JE, Tran T, Xu Y, Canan BD, Mays TA, Delfin DA, Janssen PM, Raman SV. Early treatment with lisinopril and spironolactone preserves cardiac and skeletal muscle in duchenne muscular dystrophy mice. Circulation. 2011;124:582–8. [PubMed: 21768542]

[13]. Raman SV, Hor KN, Mazur W, Halnon NJ, Kissel JT, He X, Tran T, Smart S, McCarthy B, Taylor MD, Jefferies JL, Rafael-Fortney JA, Lowe J, Roble SL, Cripe LH. Eplerenone for early cardiomyopathy in Duchenne muscular dystrophy: A randomised, double-blind, placebo-controlled trial. Lancet Neurol. 2015;14:153–61. [PubMed: 25554404]

[14]. Raman SV, Hor KN, Mazur W, He X, Kissel JT, Smart S, McCarthy B, Roble SL, Cripe LH. Eplerenone for early cardiomyopathy in Duchenne muscular dystrophy: Results of a two-year open-label extension trial. Orphanet Journal of Rare Diseases. 2017;12:39. [PubMed: 28219442]

[15]. Lowe J, Floyd KT, Rastogi N, Schultz EJ, Chadwick JA, Swager SA, Zins JG, Kadakia FK, Smart S, Gomez-Sanchez EP, Gomez-Sanchez CE, Raman SV, Janssen PM, Rafael-Fortney JA. Similar efficacy from specific and non-specific mineralocorticoid receptor antagonist treatment of muscular dystrophy mice. J Neuromusc Diseases. 2016;3:395–404.

[16]. Lowe J, Wodarcyk AJ, Floyd KT, Rastogi N, Schultz EJ, Swager SA, Chadwick JA, Tran T, Raman SV, Janssen PM, Rafael-Fortney JA. The angiotensin converting enzyme inhibitor lisinopril improves muscle histopathology but not contractile function in a mouse model of Duchenne muscular dystrophy. J Neuromusc Diseases 2015;2:257–68.

[17]. Chadwick JA, Bhattacharya S, Lowe J, Weisleder N, Rafael-Fortney JA. Renin-angiotensin-aldosterone system inhibitors improve membrane stability and change gene-expression profiles in dystrophic skeletal muscles. American Journal of Physiology Cell Physiology. 2017;312:C155–c68. [PubMed: 27881412]

[18]. Chadwick JA, Hauck JS, Gomez-Sanchez CE, Gomez-Sanchez EP, Rafael-Fortney JA. Gene expression effects of glucocorticoid and mineralocorticoid receptor agonists and antagonists on normal human skeletal muscle. Physiol Genomics. 2017;49:277–86. [PubMed: 28432191]

[19]. Chadwick JA, Hauck JS, Lowe J, Shaw JJ, Guttridge DC, Gomez-Sanchez CE, Gomez-Sanchez EP, Rafael-Fortney JA. Mineralocorticoid receptors are present in skeletal muscle and represent a potential therapeutic target. FASEB J. 2015;29:4544–54 [PubMed: 26178166]

[20]. Chadwick JA, Swager SA, Lowe J, Welc SS, Tidball JG, Gomez-Sanchez CE, Gomez-Sanchez EP, Rafael-Fortney JA. Myeloid cells are capable of synthesizing aldosterone to exacerbate damage in muscular dystrophy. Hum Mol Genet. 2016;25:5167–77. [PubMed: 27798095]

[21]. Granchelli JA, Pollina C, Hudecki MS. Pre-clinical screening of drugs using the mdx mouse. Neuromuscul Disord. 2000;10:235–9. [PubMed: 10838248]

[22]. De Luca A, Nico B, Liantonio A, Didonna MP, Fraysse B, Pierno S, Burdi R, Mangieri D, Rolland JF, Camerino C, Zallone A, Confalonieri P, Andreetta F, Arnoldi E, Courdier-Fruh I, Magyar JP, Frigeri A, Pisoni M, Svelto M, Conte Camerino D. A multidisciplinary evaluation of the effectiveness of cyclosporine a in dystrophic mdx mice. Am J Pathol. 2005;166:477–89. [PubMed: 15681831]

[23]. De Luca A, Pierno S, Liantonio A, Cetrone M, Camerino C, Fraysse B, Mirabella M, Servidei S, Ruegg UT, Conte Camerino D. Enhanced dystrophic progression in mdx mice by exercise and beneficial effects of taurine and insulin-like growth factor-1. J Pharmacol Exp Ther. 2003;304:453–63. [PubMed: 12490622]

[24]. Spurney CF, Guerron AD, Yu Q, Sali A, van der Meulen JH, Hoffman EP, Nagaraju K. Membrane sealant Poloxamer P188 protects against isoproterenol induced cardiomyopathy in dystrophin deficient mice. BMC Cardiovasc Disord. 2011;11:20. [PubMed: 21575230]

[25]. Townsend D, Blankinship MJ, Allen JM, Gregorevic P, Chamberlain JS, Metzger JM. Systemic administration of micro-dystrophin restores cardiac geometry and prevents dobutamine-induced cardiac pump failure. Mol Ther. 2007;15:1086–92. [PubMed: 17440445]

[26]. Wong BL, Mukkada VA, Markham LW, Cripe LH. Depressed left ventricular contractile reserve diagnosed by dobutamine stress echocardiography in a patient with Duchenne muscular dystrophy. J Child Neurol. 2005;20:246–8. [PubMed: 15832620]

[27]. Yue Y, Skimming JW, Liu M, Strawn T, Duan D. Full-length dystrophin expression in half of the heart cells ameliorates beta-isoproterenol-induced cardiomyopathy in mdx mice. Hum Mol Genet. 2004;13:1669–75. [PubMed: 15190010]

[28]. Lefaucheur JP, Pastoret C, Sebille A. Phenotype of dystrophinopathy in old mdx mice. Anat Rec. 1995;242:70–6. [PubMed: 7604983]

[29]. Lynch GS, Rafael JA, Hinkle RT, Cole NM, Chamberlain JS, Faulkner JA. Contractile properties of diaphragm muscle segments from old mdx and old transgenic mdx mice. The American Journal of Physiology. 1997;272:C2063–8. [PubMed: 9227435]

[30]. Strakova J, Dean JD, Sharpe KM, Meyers TA, Odom GL, Townsend D. Dystrobrevin increases dystrophin's binding to the dystrophin-glycoprotein complex and provides protection during cardiac stress. J Mol Cell Cardiol. 2014;76:106–15. [PubMed: 25158611]

[31]. Elnakish MT, Schultz EJ, Gearinger RL, Saad NS, Rastogi N, Ahmed AA, Mohler PJ, Janssen PM. Differential involvement of various sources of reactive oxygen species in thyroxin-induced hemodynamic changes and contractile dysfunction of the heart and diaphragm muscles. Free Radic Biol Med. 2015;83:252–61. [PubMed: 25795514]

[32]. Capogrosso RF, Mantuano P, Cozzoli A, Sanarica F, Massari AM, Conte E, Fonzino A, Giustino A, Rolland JF, Quaranta A, De Bellis M, Camerino GM, Grange RW, De Luca A. Contractile efficiency of dystrophic mdx mouse muscle: *In vivo* and ex vivo assessment of adaptation to exercise of functional end points. Journal of Applied Physiology (Bethesda, Md : 1985). 2017;122:828–43.

[33]. Meyers TA, Townsend D. Early right ventricular fibrosis and reduction in biventricular cardiac reserve in the dystrophin-deficient mdx heart. Am J Physiol Heart Circ Physiol. 2015;308:H303–15. [PubMed: 25485898]

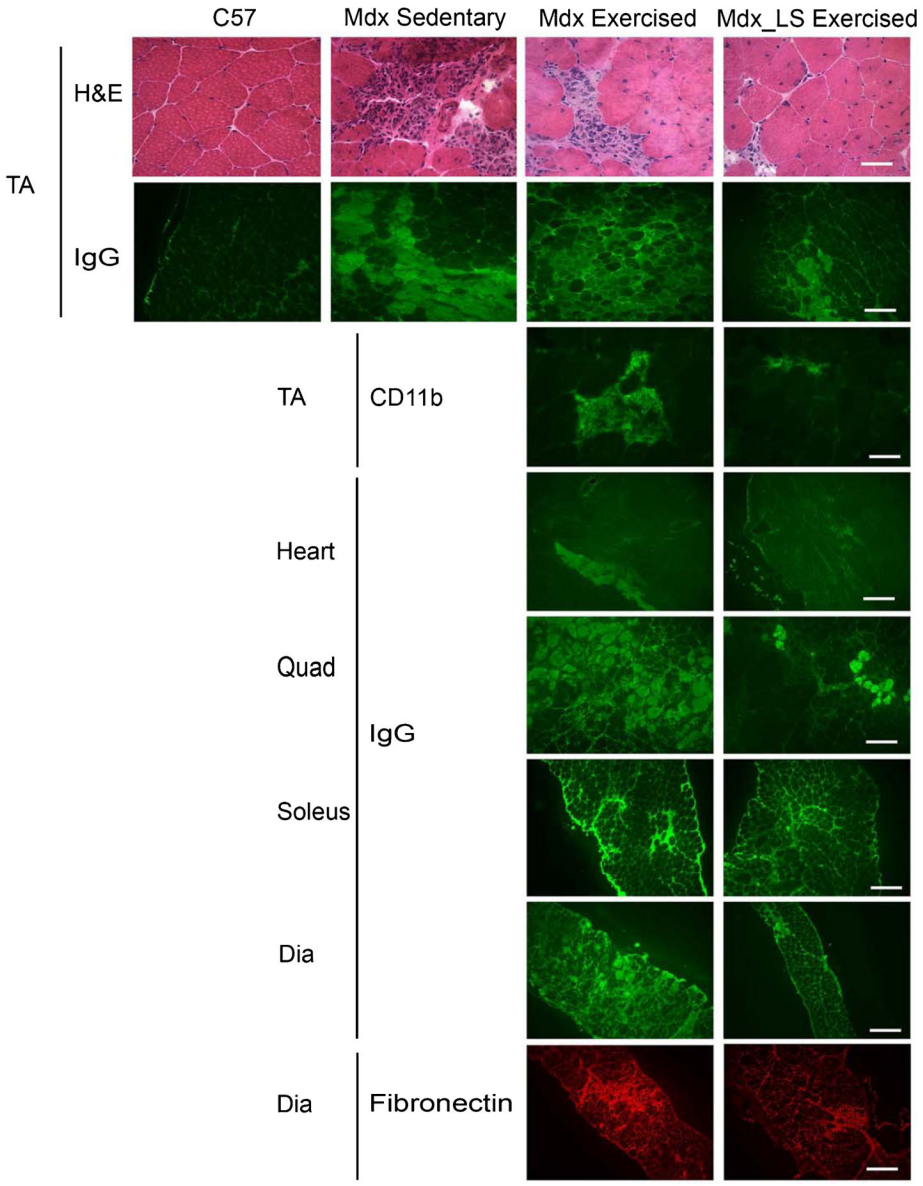

Fig. 1.

Ongoing muscle damage of mice from the Exercised *mdx* study. Representative images of TA sections from wild-type C57BL/10 (C57), *mdx* sedentary, and untreated exercised *mdx* and LS treated exercised *mdx* mice stained with H&E and IgG. Staining of immune cells for CD11b is also shown for exercised groups. Representative images of IgG staining are shown for heart, quadriceps, soleus and diaphragm sections of untreated and LS treated exercised *mdx* mice. Fibronectin staining of diaphragm sections shows fibrosis in both untreated and LS treated exercised *mdx* mice. Bar = 50 μm in CD11b, and H&E images. Bar = 200 μm in IgG and fibronectin images.

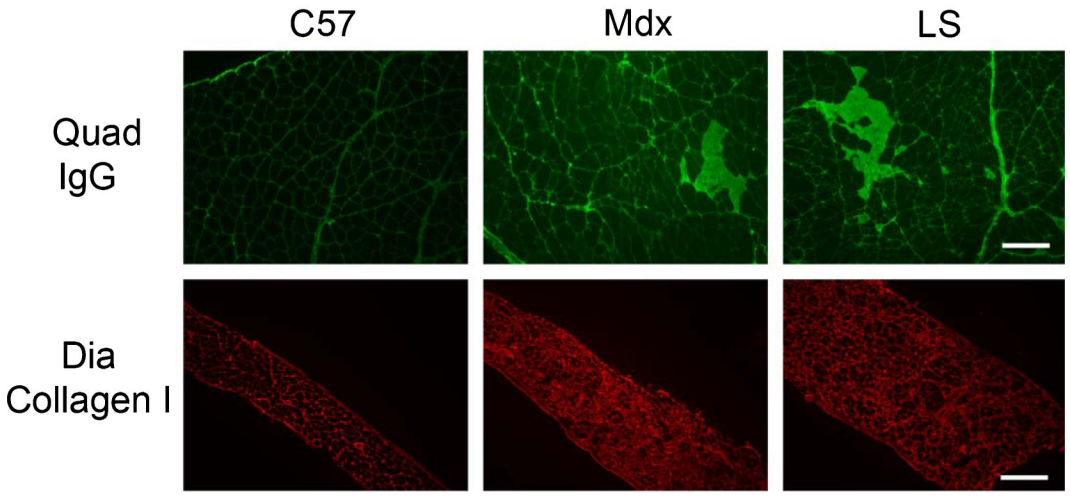

Fig. 2.

Ongoing muscle damage and fibrosis in mice from the Aged *mdx* study.

Immunofluorescence staining for IgG on representative quadriceps (Quad) sections and Collagen I on diaphragm (Dia) sections from one year-old wild-type (C57), untreated (Mdx), and LS treated *mdx* (LS) mice. Bar = 200 μm.

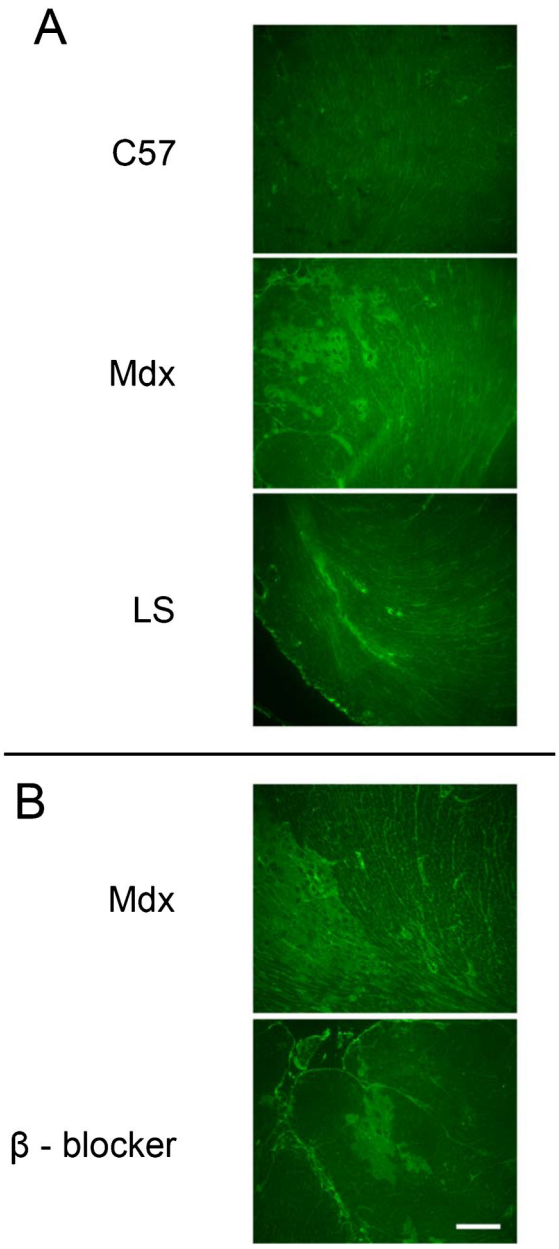

Fig. 3.

Cardiac damage in isoproterenol treated *mdx* mice. Representative images of IgG immunofluorescence on transverse heart sections through the ventricles from (A) wild-type C57, untreated *mdx*, and LS treated *mdx* after isoproterenol stress, and (B) β - blocker treated *mdx* mice with their untreated *mdx* cohort after isoproterenol stress. Bar = 200 μm.

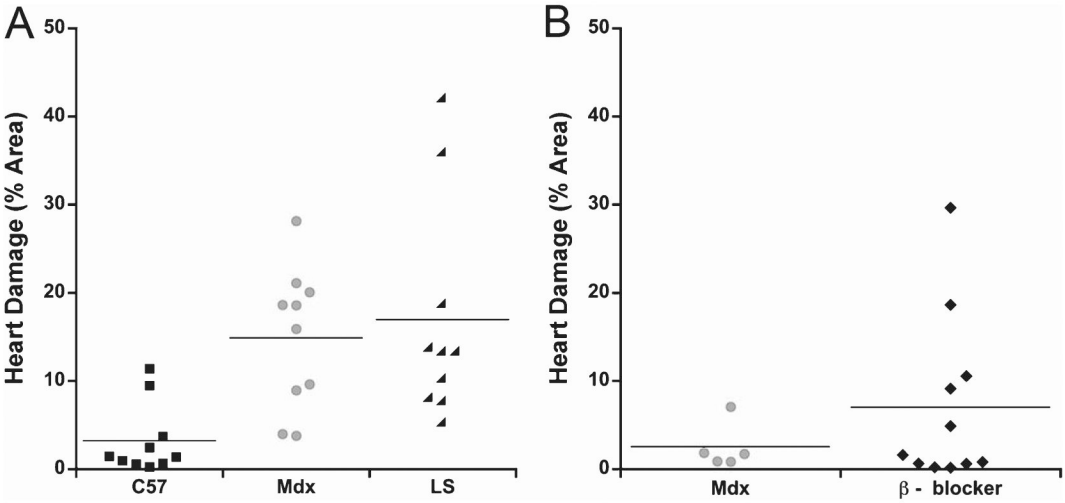

Fig. 4.

Quantification of cardiac damage in isoproterenol treated *mdx* mice. A) Dot plot showing percentage cross sectional area of IgG immunofluorescence in wild-type C57, untreated *mdx*, and LS treated *mdx* after isoproterenol stress; and B) β - blocker treated *mdx* mice with their untreated *mdx* cohort after isoproterenol stress.

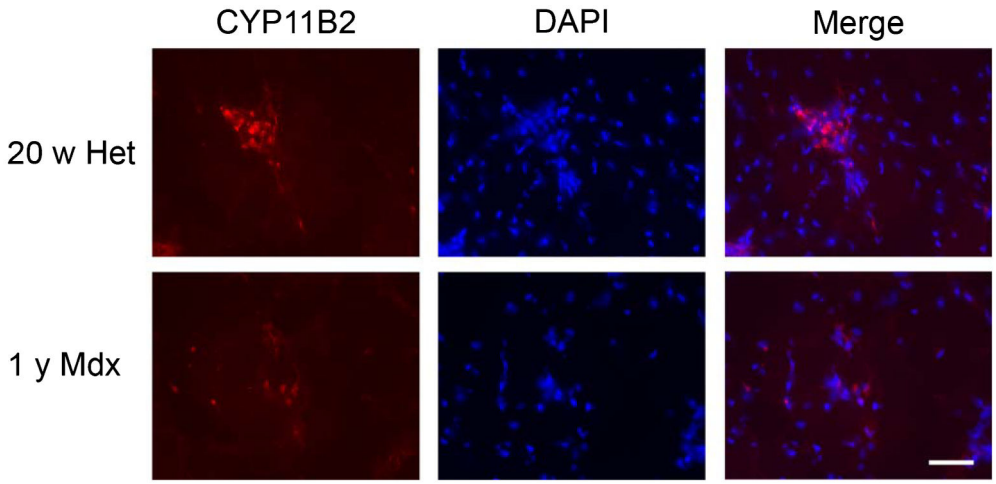

Fig. 5.

Aldosterone synthase CYP11B2 localization in young and old dystrophic mouse muscles. CYP11B2 immunofluorescence staining (red) and DAPI (blue) of quadriceps muscle sections from untreated 20 week-old *utrn*$^{+/-}$;*mdx* (Het) and 1 year-old *mdx* mice. Bar = 50 μm.

J Neuromuscul Dis. Author manuscript; available in PMC 2019 September 09.

Table 1

Exercised *mdx* study data

	Untreated *mdx* males Mean ± SEM (n)	**LS treated *mdx* males Mean ± SEM (n)**	**Student's *t*-test *P*-value**
Body Weight (BW, g)	26.4±0.7 (12)	26.7±0.8 (12)	0.8092
Grip Strength (GS) - 6 w (N)	1.5±0.07 (12)	1.5±0.10 (12)	0.6775
GS -10 w (N)	2.2±0.1 (12)	2.2±0.3 (12)	0.8156
GS/BW - 6 w (mN/g)	72.7±3.5 (12)	67.9±5.0 (12)	0.4379
GS/BW - 10 w (mN/g)	83.1±3.5 (12)	83.3±8.7 (12)	0.9831
Δ GS Exerc (mN/g)	10.4±4.2 (12)	15.4±10.6 (12)	0.6620
Heart Weight (HW, g)	0.15±0.005 (12)	0.16±0.005 (12)	0.7244
HW/BW (mg/g)	5.8±0.2 (12)	5.8±0.1 (12)	0.8956
Heart Rate (bpm)	592±16 (12)	610±22 (12)	0.5333
QT (ms)	50.3±0.8 (12)	50.1±0.9 (12)	0.8915
QTc (ms)	47.0±4.0 (12)	38.5±2.5 (12)	0.1014
Dia specific force (mN/mm^{-2})	107±17.9 (12)	111±9.6(11)	0.8487
Dia fatigue (force fraction) *	0.27±0.03 (12)	0.28±0.03 (11)	0.8232
Dia abs recov (mN/mm^{-2}) **	13.0±2.8 (12)	14.4±1.6 (11)	0.6832
Dia rel recov (%)	71.3±8.4 (12)	69.7±4.5 (11)	0.8634
EDL specific force (mN/mm^{-2})	336±58 (7)	355±35 (9)	0.7709
TA IgG (% CSA)	10±4.0 (12)	4±1.1 (12)	0.1201
TA CD11B (% CSA)	6.2±1.2 (12)	7.2±0.8 (11)	0.5098
Quad IgG (% CSA)	7±2 (12)	14±4 (12)	0.0932
Dia Fibronectin (% CSA)	11±1.1 (12)	10±1.0 (12)	0.8746
Centrally nucleated quad fibers (%)	70.8±2 (11)	70.5±1.2 (12)	0.8924

Grip strength (GS); body weight (BW); heart weight (HW); heart rate (HR); QT interval (QT); QT adjusted for heart rate variability (QTc); diaphragm (Dia); *extensor digitorum longus* (EDL); *tibiallis anterior* (TA); quadriceps (quad).

*Fraction of force left after 2 fatigue protocols, calculated by force at end of second protocol divided by force at beginning of first protocol.

**Recovery of absolute force between end of the first fatigue protocol to beginning of the second protocol.

Table 2

Aged *mdx* study data

	Control C57 males Mean ± SEM (n)	Untreated mdx males Mean ± SEM (n)	LS treated mdx males Mean ± SEM (n)	*P*-value	
				ANOVA	Dunnett Untreat vs LS
Body Weight (g)	30.6±1.4 (15)	33.0±0.7 (18)	31.7±0.9 (18)	0.2378	0.5007
Exhaustion Running (m)	870.6±189.1 (6)	270.6±25.1 (6)	262.1±46.9 (6)	0.0022	0.9979
GS Trial 1 (N)	1.4±0.06 (14)	0.9±0.03 (18)	0.9±0.05 (18)	<0.0001	0.9789
GS Trial 5 (N)	1.4±0.05 (14)	0.86±0.03 (18)	0.87±0.04 (18)	<0.0001	0.9816
GS/BW trial 1 (mN/g)	50.9±2.5 (14)	28.7±1.2(18)	30.1±1.1 (18)	<0.0001	0.7519
GS/BW trial 5 (mN/g)	49.2±2.5 (14)	26.9±0.9 (18)	27.2±1.0 (18)	<0.0001	0.9779
Heart Weight (g)	0.14±0.007 (15)	0.14±0.003 (18)	0.14±0.01 (18)	0.7038	0.6194
HW/BW (mg/g)	4.6±0.1 (15)	4.3±0.1 (18)	4.6±0.4 (18)	0.7077	0.6641
HR (bpm)	730±12.9 (8)	735±7.2 (16)	731±10.3 (15)	0.9270	0.9430
QT (ms)	44.2±1.5 (8)	42.6±0.7 (16)	44.2±0.8 (15)	0.3255	0.2992
QTc (ms)	48.2±1.2 (8)	47.0±0.7 (16)	48.7±0.7 (15)	0.2673	0.1995
Ejection fraction (%)	43.4±1.8 (8)	59.8±2.5 (8)	57.8±2.7 (8)	0.0001	0.7686
Dia spec. force (mN/mm^{-2})	150±20.4 (13)	102±7.5 (16)	98±9.2(15)	0.0123	0.9493
Dia fatigue (force fraction) *	0.28±0.03 (14)	0.36±0.02(18)	0.32±0.02(14)	0.0521	0.3461
Dia abs recov (mN/mm^{-2}) **	17±3.3 (14)	8±0.9 (18)	9±1.5 (14)	0.0035	0.8511
Dia rel recov (%)	60±7.0(14)	45±3.0(18)	47±4.0(14)	0.0457	0.8958
EDL specific force (mN/mm^{-2})	336±17 (14)	284±13 (18)	261±16 (18)	0.0056	0.4526
ECC1 (mN/mm^{-2})	323±24 (15)	269±15 (18)	250±14 (17)	0.0209	0.6594
ECC2 (% Ecc1)	94±2 (15)	87±3 (18)	90±1.5 (17)	0.0363	0.3066
ECC5 (% Ecc1)	79±5 (15)	62±6 (18)	73±3 (17)	0.0459	0.1713
Post-rest ecc6/ecc1 (% tet)	82±5 (15)	64±6 (18)	75±3 (17)	0.0348	0.1843
Quad IgG (# Fibers)	2±1 (7)	18±5 (9)	23±7 (12)	0.0779	0.8387
Dia Coll (% CSA)	25±2.0 (15)	59±2 (18)	55±3 (18)	<0.0001	0.2688

Grip strength (GS); body weight (BW); heart weight (HW); heart rate (HR); QT interval (QT); QT adjusted for heart rate variability (QTc); diaphragm (Dia); *extensor digitorum longus* (EDL); EDL force after eccentric contraction (ECC); quadriceps (quad).

* Fraction of force left after 2 fatigue protocols, calculated by force at end of second protocol divided by force at beginning of first protocol.

** Recovery of absolute force between end of the first fatigue protocol to beginning of the second protocol.